The Astrophysical Journal Letters, 802:L10 (6pp), 2015 March 20 doi:10.1088/2041-8205/802/1/L10

M DWARF LUMINOSITY, RADIUS, AND α-ENRICHMENT FROM *I*-BAND SPECTRAL FEATURES

Ryan C. Terrien[1,2,3], Suvrath Mahadevan[1,2,3], Chad F. Bender[1,2], Rohit Deshpande[1,2], and Paul Robertson[1,2]
[1] Department of Astronomy and Astrophysics, The Pennsylvania State University, 525 Davey Laboratory, University Park, PA 16802, USA; rct151@psu.edu
[2] Center for Exoplanets and Habitable Worlds, The Pennsylvania State University, University Park, PA 16802, USA
[3] The Penn State Astrobiology Research Center, The Pennsylvania State University, University Park, PA 16802, USA
Received 2014 December 23; accepted 2015 March 4; published 2015 March 23

ABSTRACT

Despite the ubiquity of M dwarfs and their growing importance to studies of exoplanets, Galactic evolution, and stellar structure, methods for precisely measuring their fundamental stellar properties remain elusive. Existing techniques for measuring M dwarf luminosity, mass, radius, or composition are calibrated over a limited range of stellar parameters or require expensive observations. We find a strong correlation between the K_S-band luminosity (M_K), the observed strength of the *I*-band sodium doublet absorption feature, and [Fe/H] in M dwarfs without strong Hα emission. We show that the strength of this feature, coupled with [Fe/H] and spectral type, can be used to derive M dwarf M_K and radius without requiring parallax. Additionally, we find promising evidence that the strengths of the *I*-band sodium doublet and the nearby *I*-band calcium triplet may jointly indicate α-element enrichment. The use of these *I*-band features requires only moderate-resolution near-infrared spectroscopy to provide valuable information about the potential habitability of exoplanets around M dwarfs, and surface gravity and distance for M dwarfs throughout the Galaxy. This technique has immediate applicability for both target selection and candidate planet–host system characterization for exoplanet missions such as *TESS* and *K2*.

Key words: planets and satellites: fundamental parameters – stars: abundances – stars: activity – stars: fundamental parameters – stars: low-mass – techniques: spectroscopic

Supporting material: machine-readable table

1. INTRODUCTION

M dwarfs account for the majority of nearby stars (e.g., Reid et al. 2002), but due to their relative faintness and complex molecular spectra, precise (<10%) measurements of their stellar parameters remain challenging. Measurements of the stellar mass, radius, luminosity, and composition of M dwarfs are important for studies of stellar structure (Torres et al. 2009), Galactic evolution (Bochanski et al. 2013), and particularly for studies of exoplanets, since indirectly derived planetary characteristics and histories depend on accurate knowledge of the host star. M dwarfs are attractive planet search targets because their smaller sizes and lower luminosities result in larger radial velocity (RV) and transit depth signatures compared to Sun-like stars. They appear to host numerous planetary systems (Dressing & Charbonneau 2015) and are prioritized in planned exoplanet surveys (e.g., Ricker et al. 2015). However, the characterization of the resulting planets and whether they are in the habitable zone (Kasting 1993) could be clouded by lack of efficient and precise stellar characterization.

The complexity of M dwarf spectra encumbers spectroscopic modeling and the measurement of stellar parameters. Numerous techniques have been developed to circumvent this difficulty, by relating M dwarf parameters to easily measured photometry or moderate-resolution spectroscopic features. These relations are calibrated using stars for which the parameters are known a priori, such as M dwarfs with interferometrically measured radii (Boyajian et al. 2012; Mann et al. 2013b; Newton et al. 2015) or M dwarf companions to higher-mass stars with well-measured compositions (e.g., Bonfils et al. 2005; Johnson & Apps 2009; Rojas-Ayala et al. 2012; Mann et al. 2013a; Newton et al. 2014).

Determinations of M dwarf radius, luminosity, and mass can be made through empirical relations between these parameters and M dwarf effective temperature ($T_{\rm eff}$), which can be estimated from moderate-resolution spectral features (Boyajian et al. 2012; Mann et al. 2013b). However, this technique is limited by systematic errors when using stellar models to predict M dwarf parameters from $T_{\rm eff}$ and [Fe/H] (e.g., Boyajian et al. 2012), by the paucity of interferometric calibrator stars, and by a large range of M dwarf parameters at a given estimated $T_{\rm eff}$ (e.g., Newton et al. 2015). Combining improved $T_{\rm eff}$ measures and [Fe/H] enables better M dwarf parameters, but requires broadband flux-calibrated spectra (Mann et al. 2015).

One can also estimate M dwarf parameters from K_s-band luminosity (M_K), which is well correlated with stellar mass and insensitive to metallicity (Delfosse et al. 2000). This allows mass measurements of nearby M dwarfs with parallaxes, but parallaxes for many nearby M dwarfs may not be available for several years (Perryman et al. 2001). For M dwarfs without parallax measurements, some success has been achieved in determining M_K using high-resolution spectra (Pineda et al. 2013), but such spectra are observationally expensive. Methods that do not require parallax, high-resolution spectra, or absolute flux measurements of the target stars, and which can be applied immediately are highly desirable.

We have developed a simple, powerful technique, based on the strengths of the *I*-band neutral sodium doublet (~820 nm, hereafter Na I) and singly ionized calcium triplet (~860 nm, hereafter Ca II), to enable determination of M dwarf M_K and radius and convey information about M dwarf surface gravity and possibly α-enrichment. We present here an observational study that shows the potential applicability of these *I*-band features in conjunction with measurements of M dwarf $T_{\rm eff}$ and [Fe/H], all obtained from moderate-resolution near-infrared spectra.

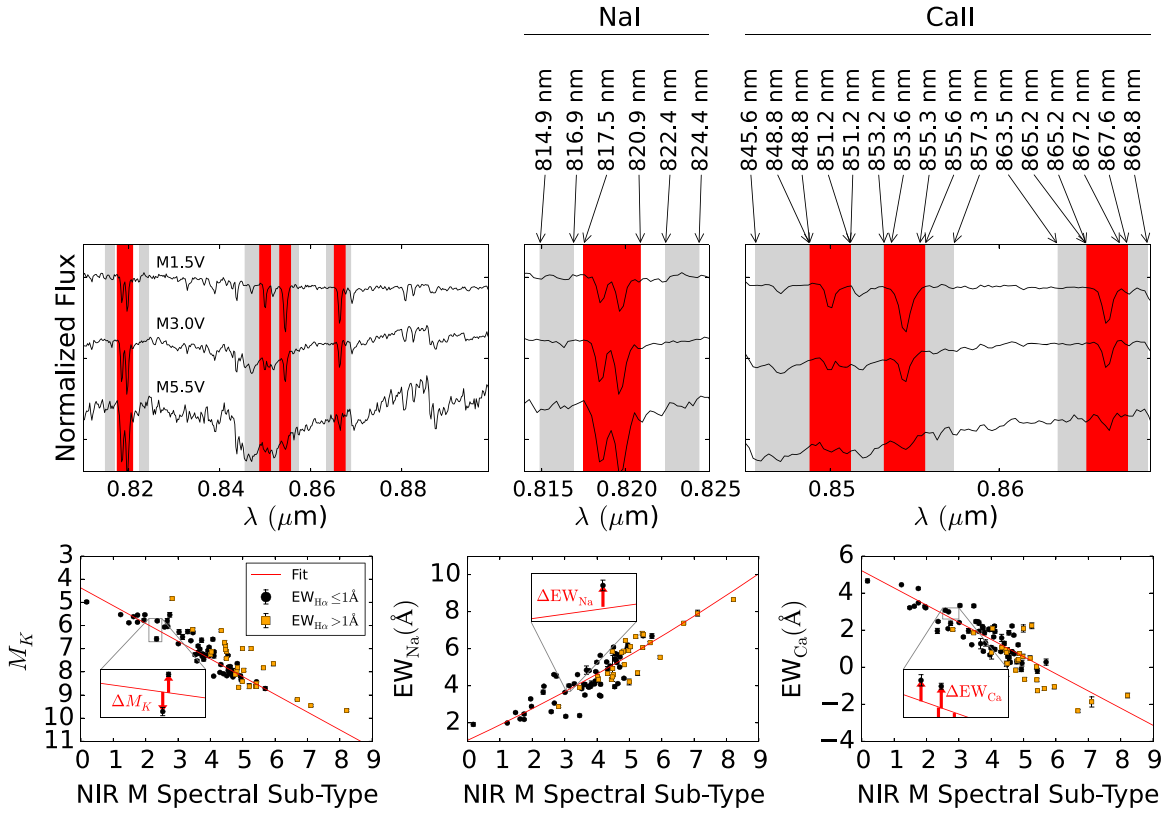

Figure 1. Top: the feature (red) and continuum (gray) definitions for the quantities used in this work. Bottom: the strengths of the features with NIR M subtype (a proxy for $T_{\rm eff}$). For Na I, Ca II, and M_K, we fit a low-order polynomial to these quantities for a subset of M dwarfs in our sample and defined $\Delta{\rm EW_{Na}}$, $\Delta{\rm EW_{Ca}}$, ΔM_K as the departure from this fit (see Section 2).

2. OBSERVATIONS AND METHODS

The 342 stars used here were observed in our IRTF-SpeX (Rayner et al. 2003) M dwarf survey. Terrien et al. (2012) detailed the observations and data reduction. We also include spectra of nine nearby M dwarfs from Mann et al. (2013b). All spectra have $R \sim 2000$ and span 0.8–2.4 μm. We measured [Fe/H] for each star using the weighted (by signal-to-noise ratio, S/N) average of the J, H, K_s near-IR (NIR) spectral calibrations of Mann et al. (2013a; for M5 and earlier) and Mann et al. (2014; later than M5), which have <0.1 dex precision. We also measured the $T_{\rm eff}$-sensitive H_2O-K2 index and associated NIR M spectral type (NIR SpT) explored in Rojas-Ayala et al. (2012) and Newton et al. (2014).

For each target, we compiled parallax (from the RECONS[4] database; van Altena et al. 1995; Gould & Chaname 2004; van Leeuwen 2007; Gatewood 2008; von Braun et al. 2011; Anglada-Escudé et al. 2012; Dittmann et al. 2014), proper motion (Zacharias et al. 2013), and RV (Chubak et al. 2012; Newton et al. 2014) where available. We used Hα equivalent width measurements (e.g., Gizis et al. 2002; Riaz et al. 2006; Gaidos et al. 2014) to constrain activity levels for our M dwarfs.

Our technique relies on measurements of the pseudo-equivalent widths (EWs) of the Na I and Ca II features. The Na I doublet is a known gravity indicator for M dwarfs (Schiavon et al. 1997; Martín et al. 2010; Schlieder et al. 2012), and both the Na I doublet and the Ca II triplet have shown possible sensitivity to Hα-based activity levels (Kafka & Honeycutt 2006). The definitions of the features and continuum regions are shown in Figure 1. For the Na I doublet and each component of the Ca II triplet, we fit a line to the two neighboring continuum regions (Figure 1), and calculated the EW of the feature relative to this line. Our final $\rm EW_{Ca}$ value is the sum of the three components. We define positive EW as absorption for the Ca II and Na I features. The measured and literature parameters for each star are listed in Table 1. For six M dwarfs observed in our program and Mann et al. (2013b), we find no offset for the Na I feature, but that our measurements of $\rm EW_{Ca}$ are systematically 0.96 Å higher, possibly due to our use of SpeX ($R \sim 2000$) in the I-band instead of SNIFS (Lantz et al. 2004; $R \sim 1000$) used in Mann et al. (2013b). We apply this correction for the nine stars from Mann et al. (2013b) that are not in our sample.

To explore the empirical behavior of M_K, $\rm EW_{Na}$, and $\rm EW_{Ca}$ as a function of NIR SpT, we used a subset of 84 M dwarfs with high S/N spectra, parallax measurements with precisions better than 5%, no indications of multiplicity, and either low ($\rm EW_{H\alpha} < 1$ Å, $n = 57/84$) or high ($\rm EW_{H\alpha} \geqslant 1$ Å, $n = 27/84$) activity levels as evidenced by the strength of Hα emission (e.g., West et al. 2004). We fit each of these quantities with a low-order polynomial as shown in Figure 1, and defined ΔM_K, $\Delta{\rm EW_{Na}}$, and $\Delta{\rm EW_{Ca}}$ as the departure from these fits at a given NIR SpT. For M_K and Ca II, we used only the low-activity subset ($n = 57$), as these stars exhibit structural changes related to activity (Stassun et al. 2012, and references therein) and we observe the Ca II feature in emission in some M dwarfs. We used all 84 stars for the fit to $\rm EW_{Na}$, because there is no clear evidence of activity measurably affecting the strength of the

[4] http://www.recons.org

Table 1
M Dwarf Parameters and Measurements

2MASS ID	[Fe/H]	NIR SpT	EW_{Na} (Å)	EW_{Ca} (Å)	$R_{interfer.}$[a] ($R_\odot$)	R_π[b] ($R_\odot$)	R_{Na}[c] ($R_\odot$)	M13 Flag[d]
00064325−0732147	−0.11	5.99	7.46 ± 0.05	0.24 ± 0.07	…	…	…	…
00085391+2050252	0.00	4.93	5.38 ± 0.11	0.83 ± 0.15	…	…	…	…
00115302+2259047	0.15	3.62	4.08 ± 0.09	2.38 ± 0.11	…	…	…	…
00165629+0507261	−0.14	4.52	3.90 ± 0.09	1.80 ± 0.11	…	…	…	…
00182256+4401222	−0.26	1.89	2.56 ± 0.10	4.45 ± 0.13	0.386 ± 0.002	0.395 ± 0.004	0.416 ± 0.027	…
00182549+4401376	−0.09	4.10	5.64 ± 0.05	2.22 ± 0.08	…	…	…	…
00283948−0639481	−0.11	4.18	3.25 ± 0.14	2.01 ± 0.15	…	…	…	…
00313539−0552115	−0.12	3.68	4.06 ± 0.09	2.12 ± 0.13	…	…	…	…
00321574+5429027	−0.05	4.49	3.85 ± 0.07	1.55 ± 0.10	…	…	…	…
00383388+5127579	−0.24	2.83	3.30 ± 0.07	3.25 ± 0.09	…	…	…	…

[a] Interferometric radius from Boyajian et al. (2012).
[b] Interpolated at parallax-based M_K and 5 Gyr age in Dartmouth model grid.
[c] Interpolated at predicted M_K (see Section 3.1) in Dartmouth model grid.
[d] Spectrum from Mann et al. (2013b).

(This table is available in its entirety in machine-readable form.)

Na I feature in our data. The resulting definitions and low-order fits are

$$\Delta EW_{Na} = EW_{Na} - (1.07 + 0.78\,[\text{NIR SpT}] + 0.03\,[\text{NIR SpT}]^2), \quad (1)$$

$$\Delta EW_{Ca} = EW_{Ca} - (5.23 - 0.93\,[\text{NIR SpT}]), \quad (2)$$

$$\Delta M_K = M_K - (4.36 - 0.77\,[\text{NIR SpT}]). \quad (3)$$

3. RESULTS AND DISCUSSION

3.1. A Relationship between M_K, EW_{Na}, and [Fe/H]

We find that a first-order linear model based on ΔEW_{Na} and [Fe/H] yields an excellent predictor of ΔM_K (Figure 2(*A*)) in the low-activity subset. The resulting equation is

$$\Delta M_K = -1.66\,[\text{Fe/H}] + 0.55\,\Delta EW_{Na} - 0.11, \quad (4)$$

which has an adjusted squared correlation coefficient $R^2 = 0.64$ and residual scatter of 0.18 mag (excluding two overluminous stars that we suspect are binaries: 2MASS J04223199+1031188, 2MASS J02532611+1724324; Figure 2(*B*)). This approximately halves the intrinsic ∼0.35 mag scatter in M_K from NIR SpT (Figure 1). We explored alternative definitions of the Na I features (Martín et al. 2010; Schlieder et al. 2012), and the quality of the resulting fits differs negligibly from that reported here.

This model directly reveals that EW_{Na} is sensitive to small changes in M_K at a given NIR SpT. This is primarily due to the strong sensitivity of this feature to surface gravity at low T_{eff}, a behavior that has been thoroughly explored in the context of youth indicators for low-mass stars (Schlieder et al. 2012). With the inclusion of [Fe/H] in our model, we disentangle the gravity and [Fe/H] sensitivity of the Na I feature, which goes from being a binary indicator of youth or low gravity to having a much finer sensitivity to luminosity and surface gravity. Thus, this feature is a precise and easily measured gravity indicator for M dwarfs, a stellar regime in which established precision gravity measurement techniques (e.g., Bastien et al. 2013) are not yet applicable.

Our interpretation that the ΔM_K–ΔEW_{Na} –[Fe/H] relationship results from the gravity-sensitivity of EW_{Na} depends on the observed insensitivity to gravity of our [Fe/H] measurements. Although the Mann et al. (2013a) [Fe/H] calibrations employ gravity-sensitive features, we note that the ΔM_K–ΔEW_{Na} –[Fe/H] relationship is present (with similar coefficients) with different indicators of [Fe/H] (e.g., the individual *H*- and *K*-band calibrations), which are based on different features with varied behaviors with gravity. We also find this relationship using [Fe/H] derived from higher-mass companions, which are available for 21 of our stars from Valenti & Fischer (2005), and which are immune to effects within the M dwarf spectrum. We conclude that gravity-related systematic errors in our [Fe/H] measurements are insignificant.

We considered that our NIR SpT measurements could similarly have systematic errors that impact our interpretation of the ΔM_K–ΔEW_{Na} –[Fe/H] relationship. We note that our NIR SpTs are based on the H_2O-K2 index, which is known to correlate with T_{eff} to <80 K (e.g., Mann et al. 2013b). By contrast, the ΔM_K–ΔEW_{Na} –[Fe/H] relationship extends over ∼1.5 mag in ΔM_K, which would equate to many hundreds of degrees in T_{eff}. We conclude that, within their stated errors, our [Fe/H] and T_{eff} indicators are accurately accounting for their contribution to the behavior of EW_{Na}. Therefore, the well-established gravity-sensitivity of EW_{Na} is the most reasonable explanation for its correlation with ΔM_K.

This model efficiently provides M_K for M dwarfs without parallaxes, thereby enabling "spectroscopic distance" and fundamental parameter measurements of M dwarfs. As an illustration, we note that for one of the best-characterized M dwarfs in the *Kepler* sample, *Kepler* 138 (KOI 314), we predict $M_K = 5.42 \pm 0.18$ based on a single moderate-resolution NIR spectrum. This is in excellent agreement with the $M_K = 5.39 \pm 0.25$ measured in Pineda et al. (2013), which is based on six high-resolution spectra of this star and library of more than 100 similar high-S/N spectra. Through the tight relations between M_K and stellar mass (e.g., Delfosse et al. 2000) and radius, the model we present can help to provide determinations of M dwarf parameters and the location of the habitable zone for M dwarf exoplanet hosts.

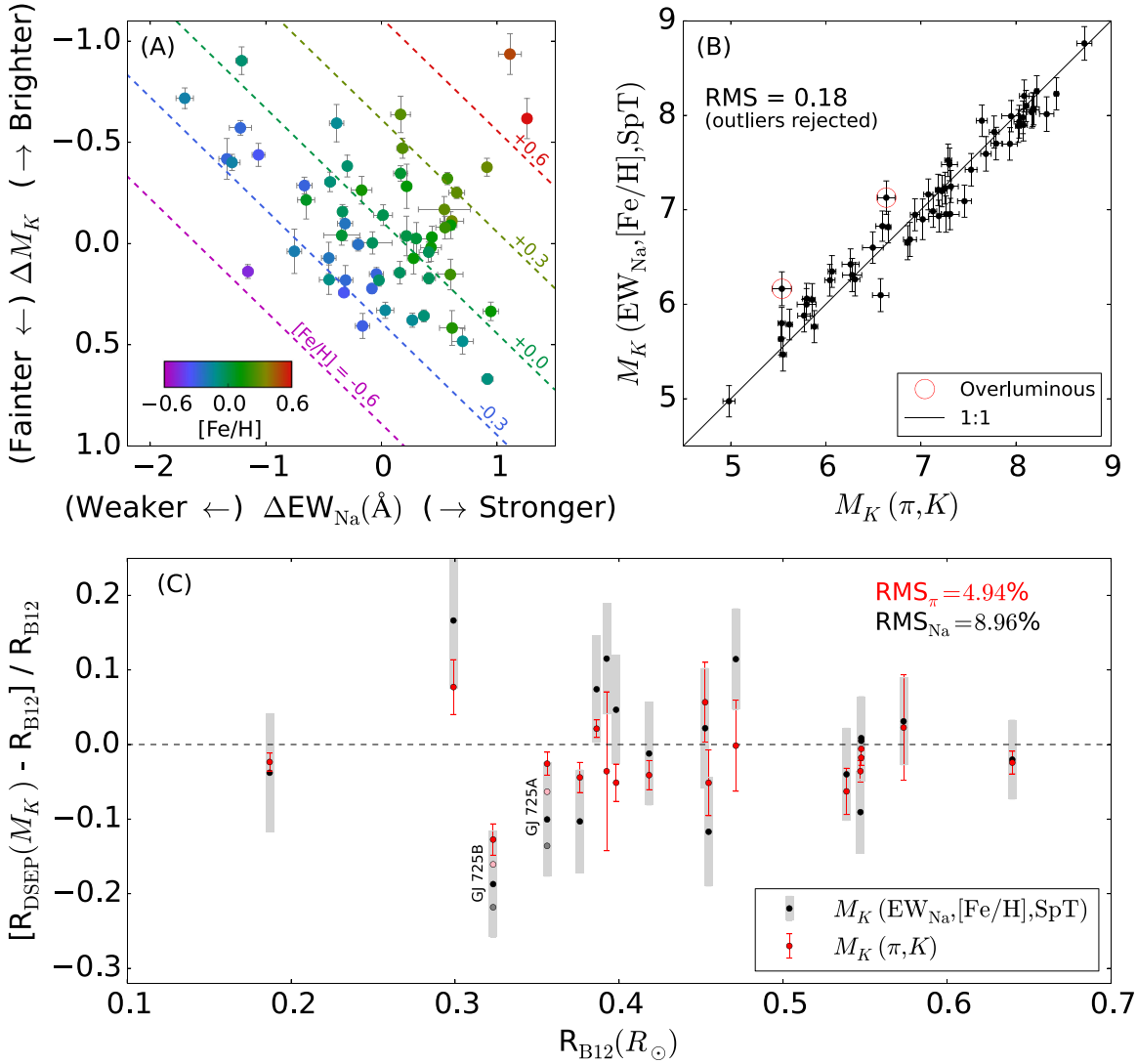

Figure 2. (A) For 57 well-characterized nearby M dwarfs, the relationship between ΔM_K, ΔEW_{Na}, and [Fe/H], along with iso-[Fe/H] contours from our model that predicts ΔM_K from ΔEW_{Na} and [Fe/H]. (B) For the same set of stars, the known parallax (π)-based M_K and our predicted M_K based on EW_{Na}, [Fe/H] and NIR SpT. A 1:1 relation is shown; two overluminous targets that are likely binaries are highlighted. (C) For 18 M dwarfs with interferometrically measured radii (Boyajian et al. 2012), the fractional difference between the calculated (R_{DSEP}) and measured radii (R_{B12}). To derive radius, we interpolate on the Dartmouth model grid at an M_K and [Fe/H] appropriate to each star. We used two different values for M_K for each star: the measured parallax (π)-based M_K (black, gray error bars) and the M_K predicted from our calibration of the Na I doublet (red). The R values from predicted M_K values have $rms_{Na} \approx 9\%$, compared to $rms_\pi \approx 5\%$ from parallax-based M_K. We note that the mean error in R_{B12} is ~2%. Both sets of radii measurements are consistent with <2% offset from the Dartmouth models. GJ 725, a system with Ca II and Na I feature strengths suggestive of α-enrichment, is highlighted; the Dartmouth models with $[\alpha/Fe] = +0.2$ are shown in black and red while the $[\alpha/Fe] = 0.0$ results are indicated in gray and pink (Dotter et al. 2008) explains details regarding α-enrichment in the Dartmouth models). For all other systems we used $[\alpha/Fe] = 0.0$.

Compared with existing techniques for measuring these parameters (Mann et al. 2013b; Newton et al. 2015), our technique benefits from a large set of calibrators, and requires only a single, non-flux calibrated, moderate-resolution NIR spectrum.

3.2. M Dwarf Radius from M_K

After establishing that the Na I feature, [Fe/H], and NIR SpT can be used to determine M dwarf M_K, we explored extending the technique to measuring M dwarf radius, using 18 nearby M dwarfs with interferometrically measured radii (Figure 2(C)). We interpolated the Dartmouth Stellar Evolution Program (Dotter et al. 2008) models at the [Fe/H] and M_K of each star to predict radius, using both the parallax-based M_K and the spectroscopic M_K indicated by the techniques in Section 3.1. We compared these radii with the interferometric radii (Boyajian et al. 2012). We note that the mean error in the interferometrically measured radii themselves is approximately 2%. We found that we could derive radius to ~5% when using the parallax-based M_K, and to ~10% with just the information available from the NIR spectra. We find no evidence for $a > 2\%$ systematic offset between M_K-based model-predicted and measured M dwarf radii in these 18 stars, in contrast to interpolations at L_{Bol} and T_{eff} (e.g., Section 5 of Boyajian et al. 2012), demonstrating the advantages of using M_K and a possible path toward reconciling low-mass stellar models and observations. Using M_K to derive radius is therefore an accurate, precise, and efficient method that can be applied to M dwarfs well beyond the reach of current interferometric facilities.

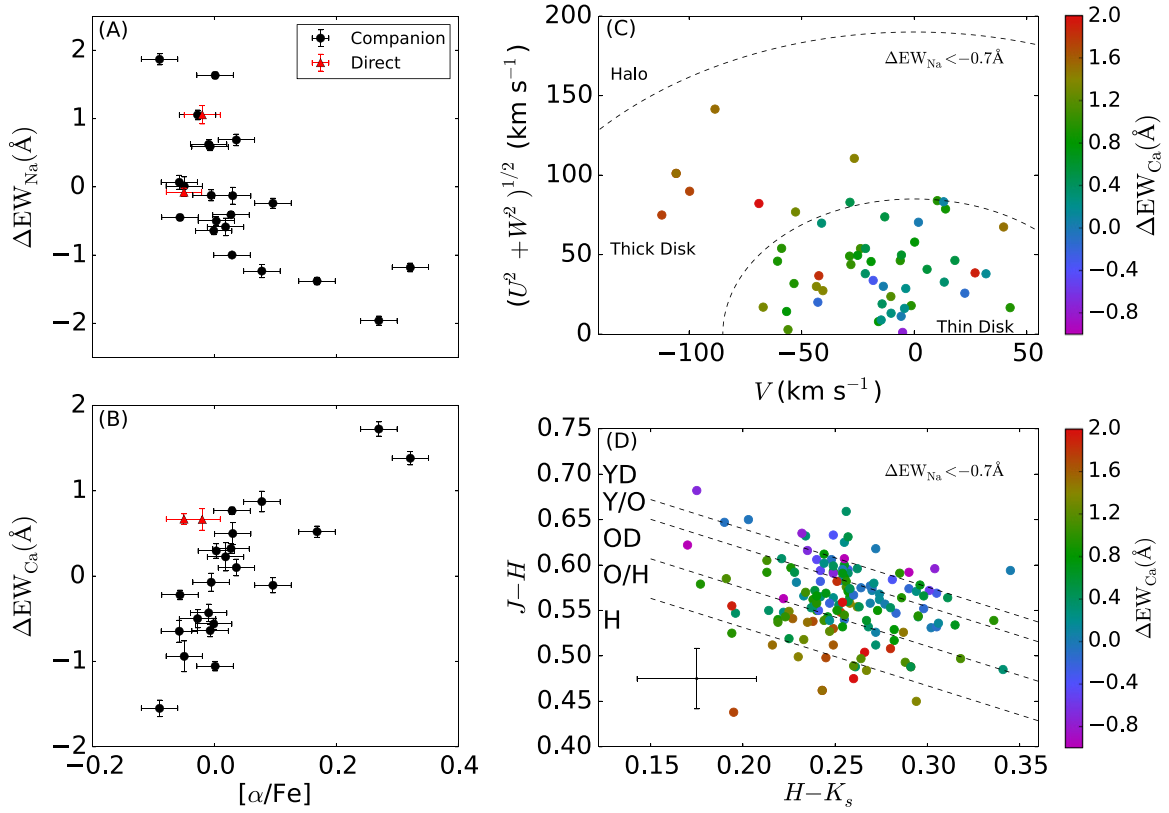

Figure 3. The behavior of the Ca II and Na I features with α-enrichment. (A, B) For 23 M dwarfs, the reported $[\alpha/Fe]$ parameter is the weighted averages of literature measurements of [Si/Fe] and [Ti/Fe] of a higher-mass common proper motion companion or the M dwarf itself, as a function of ΔEW_{Na} and ΔEW_{Ca}. High ΔEW_{Ca} and low ΔEW_{Na} are clearly associated with α-enrichment. (C) The Toomre diagram for M dwarfs with well-measured UVW velocities, and nominal Galactic population boundaries. Stars that are dynamically consistent with being old also have high ΔEW_{Ca}. (D) The color–color diagram with delineations of different populations (Leggett 1992). M dwarfs with high ΔEW_{Ca} have colors consistent with old ages.

3.3. Measurements of M Dwarf α-enrichment?

The α-elements, such as silicon and titanium, can be formed in SNe II, and they are more abundant ("enriched") relative to iron in older stellar populations. To explore the sensitivity of the Na I and Ca II features to α-enrichment, we first considered a subset of 23 M dwarfs from our sample with α-enrichment ([Ti/Fe] and [Si/Fe]) measurements in the literature from either direct spectroscopy (Woolf & Wallerstein 2005; Chavez & Lambert 2009) or based on spectroscopy of higher-mass companions (Valenti & Fischer 2005). We found that (Figures 3 (*A*), (*B*)) α-enriched stars have higher (stronger absorption) ΔEW_{Ca} and lower (weaker absorption) ΔEW_{Na}, as expected since calcium is an α-element and sodium is not. Moreover, for the subset of our M dwarfs where measurements are available, high ΔEW_{Ca} and low ΔEW_{Na} are also consistent with kinematic and color-based indicators of old age. A Toomre diagram (Figure 3(*C*), Sandage & Fouts 1987), which shows stellar Galactocentric vertical (U^2), radial (W^2), and rotational (V^2) kinetic energies, can dynamically separate older and younger stars: older stars have a wide distribution of kinetic energies, while younger stars have lower kinetic energies. The lower metallicities of older stars also separate these stars well in the $(J-H, H-K)$ color–color plane (Figure 3(*D*)), due to H^- continuum and H_2O opacity effects (Leggett 1992). These observational indications of abundance and age suggest that the Na I and Ca II features jointly indicate α-enrichment in M dwarfs.

Figure 4 shows the plane defined by ΔEW_{Na} and ΔEW_{Ca}. We note that, for the lowest ΔEW_{Na} values, targets with low and high Hα are generally well-separated by ΔEW_{Ca} (with the exception of CM Dra, an active close binary system). This is consistent with the behavior of ΔEW_{Ca} being dominated by chromospheric activity, which is supported by our observation of Ca II in emission and the findings of Kafka & Honeycutt (2006). We also note that CM Dra, a system that is suspected of α-enrichment (Feiden & Chaboyer 2014), stands out in this plane, as does the binary system GJ 725. In both systems, models with $[\alpha/Fe] = 0.2$ provide a better match to observations than models with $[\alpha/Fe] = 0.0$ (e.g., Figure 2). We posit a simple interpretation of these features: stars with low ΔEW_{Na} are likely either low-gravity or α-enriched, and the activity-sensitivity of ΔEW_{Ca} can differentiate between these younger (more active) or older (less active) populations. As we only probe a limited range of $[\alpha/Fe]$ and [Fe/H], this interpretation is not conclusive, but is strongly suggestive and provides a promising direction for further exploration and the development of better techniques for measuring M dwarf compositions.

4. CONCLUSION

The Ca II and Na I spectroscopic indicators provide a wealth of new and easily obtained information about M dwarf stellar properties. The broad applicability of these physically motivated indicators and associated techniques in mid- to late-type

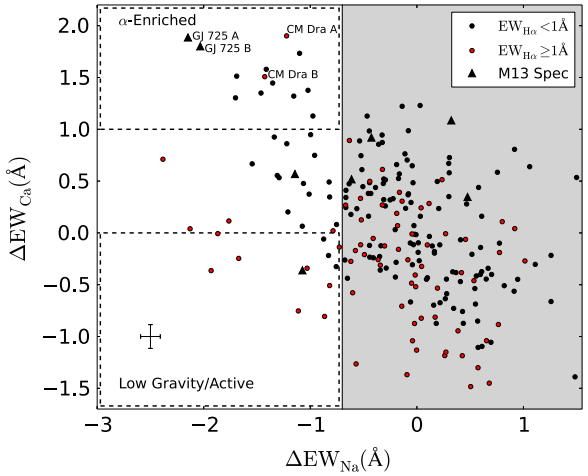

Figure 4. ΔEW_{Ca} and ΔEW_{Na} values for M dwarfs in our sample, color-coded by their level of activity as indicated by Hα. We posit a simple interpretation: stars with low ΔEW_{Na} are likely either low-gravity and young, or α-enriched and old, and ΔEW_{Ca} can discriminate between these two due to filling-in related to chromospheric activity. Two M dwarf systems (CM Dra and GJ 725) with possible α-enrichment (Feiden & Chaboyer 2014) are highlighted. Measurements on spectra from Mann et al. (2013b) are indicated separately and have been corrected for the use of a different instrument (0.96 Å offset). Mean errors for the stars observed in our program are indicated by the error bars in the lower left.

M dwarfs, their possible constraints on α-enrichment, and their simplicity offer a substantial improvement over existing methods for measuring M dwarf parameters. These indicators and techniques will be useful for appraising M dwarf planetary systems discovered in the coming years (e.g., by *TESS* and *K2*), and for prioritizing nearby M dwarf exoplanet systems for planetary atmospheric characterization with *James Webb Space Telescope*. By providing stellar mass, luminosity, and radius through M_K, they will provide a necessary foothold for measuring planetary parameters and the location of the habitable zone. They also provide a path toward more precise distances to Galactic M dwarfs, for which the current limiting factor is the scatter in the color–luminosity relations used to estimate distance (e.g., Bochanski et al. 2013). The Sloan Digital Sky Survey bandpass contains the Ca II and Na I *I*-band features, as well as indicators of metallicity and $T_{\rm eff}$ (West et al. 2011; Dhital et al. 2012), potentially enabling archival analysis with the Na I and Ca II indicators. Finally, we note that the Ca II feature will be observed by the *Gaia* RV Spectrometer and may provide leverage for the measurement of α-enrichment and activity levels in the large sample of M dwarfs observed by *Gaia*. The measurement of the features described here is relatively observationally inexpensive: a single $R \sim 2000$ NIR spectrum is sufficient, and is substantially easier to obtain than the parallax measurements, high-resolution spectra, or broadband flux-calibrated spectra required by other techniques.

This work was partially supported by funding from the Center for Exoplanets and Habitable Worlds. The Center for Exoplanets and Habitable Worlds is supported by the Pennsylvania State University, the Eberly College of Science, and the Pennsylvania Space Grant Consortium. This work was also partially supported by the Penn State Astrobiology Research Center and the National Aeronautics and Space Administration (NASA) Astrobiology Institute (NNA09-DA76A). We acknowledge support from NSF grants AST 1006676, AST 1126413, and AST 1310885. This work was partially based on data from the Infrared Telescope Facility. The Infrared Telescope Facility is operated by the University of Hawaii under Cooperative Agreement No. NNX-08AE38A with the National Aeronautics and Space Administration, Science Mission Directorate, Planetary Astronomy Program.

REFERENCES

Anglada-Escudé, G., Boss, A. P., Weinberger, A. J., et al. 2012, ApJ, 746, 37
Bastien, F. A., Stassun, K. G., Basri, G., & Pepper, J. 2013, Natur, 500, 427
Bochanski, J. J., Savcheva, A., West, A. A., & Hawley, S. L. 2013, AJ, 145, 40
Bonfils, X., Delfosse, X., Udry, S., et al. 2005, A&A, 442, 635
Boyajian, T. S., von Braun, K., van Belle, G., et al. 2012, ApJ, 757, 112
Chavez, J., & Lambert, D. L. 2009, ApJ, 699, 1906
Chubak, C., Marcy, G., Fischer, D. A., et al. 2012, arXiv:1207.6212
Delfosse, X., Forveille, T., Ségransan, D., et al. 2000, A&A, 364, 217
Dhital, S., West, A. A., Stassun, K. G., et al. 2012, AJ, 143, 67
Dittmann, J. A., Irwin, J. M., Charbonneau, D., & Berta-Thompson, Z. K. 2014, ApJ, 784, 156
Dotter, A., Chaboyer, B., Jevremović, D., et al. 2008, ApJS, 178, 89
Dressing, C. D., & Charbonneau, D. 2015, ApJ, submitted (arXiv:1501.01623)
Feiden, G. A., & Chaboyer, B. 2014, A&A, 571, A70
Gaidos, E., Mann, A. W., Lepine, S., et al. 2014, MNRAS, 443, 2561
Gatewood, G. 2008, AJ, 136, 452
Gizis, J. E., Reid, I. N., & Hawley, S. L. 2002, AJ, 123, 3356
Gould, A., & Chaname, J. 2004, ApJS, 150, 455
Johnson, J. A., & Apps, K. 2009, ApJ, 699, 933
Kafka, S., & Honeycutt, R. K. 2006, AJ, 132, 1517
Kasting, J. 1993, Icar, 101, 108
Lantz, B., Aldering, G., Antilogus, P., et al. 2004, Proc. SPIE, 5249, 146
Leggett, S. K. 1992, ApJS, 82, 351
Mann, A. W., Brewer, J. M., Gaidos, E., Lépine, S., & Hilton, E. J. 2013, AJ, 145, 52
Mann, A. W., Deacon, N. R., Gaidos, E., et al. 2014, AJ, 147, 160
Mann, A. W., Feiden, G. A., Gaidos, E., & Boyajian, T. 2015, ApJ, submitted (arXiv:1501.01635)
Mann, A. W., Gaidos, E., & Ansdell, M. 2013, ApJ, 779, 188
Martín, E. L., Phan-Bao, N., Bessell, M., et al. 2010, A&A, 517, A53
Newton, E. R., Charbonneau, D., Irwin, J., et al. 2014, AJ, 147, 20
Newton, E. R., Charbonneau, D., Irwin, J., & Mann, A. W. 2015, ApJ, 800, 85
Perryman, M. A. C., de Boer, K. S., Gilmore, G., et al. 2001, A&A, 369, 339
Pineda, J. S., Bottom, M., & Johnson, J. A. 2013, ApJ, 767, 28
Rayner, J. T., Toomey, D. W., Onaka, P. M., et al. 2003, PASP, 115, 362
Reid, I. N., Gizis, J. E., & Hawley, S. L. 2002, AJ, 124, 2721
Riaz, B., Gizis, J. E., & Harvin, J. 2006, AJ, 132, 866
Ricker, G. R., Winn, J. N., Vanderspek, R., et al. 2015, JATIS, 1, 014003
Rojas-Ayala, B., Covey, K. R., Muirhead, P. S., & Lloyd, J. P. 2012, ApJ, 748, 93
Sandage, A., & Fouts, G. 1987, AJ, 93, 592
Schiavon, R. P., Barbuy, B., Rossi, S. C. F., & Milone, A. 1997, ApJ, 479, 902
Schlieder, J. E., Lépine, S., Rice, E., et al. 2012, AJ, 143, 114
Stassun, K. G., Kratter, K. M., Scholz, A., & Dupuy, T. J. 2012, ApJ, 756, 47
Terrien, R. C., Mahadevan, S., Bender, C. F., et al. 2012, ApJL, 747, L38
Torres, G., Andersen, J., & Giménez, A. 2009, A&ARv, 18, 67
Valenti, J. A., & Fischer, D. A. 2005, ApJS, 159, 141
van Altena, W. F., Lee, J. T., & Hoffleit, D. 1995, yCat, 1174, 0
van Leeuwen, F. 2007, A&A, 474, 653
von Braun, K., Boyajian, T. S., Kane, S. R., et al. 2011, ApJ, 729, L26
West, A. A., Hawley, S. L., Walkowicz, L. M., et al. 2004, AJ, 128, 426
West, A. A., Morgan, D. P., Bochanski, J. J., et al. 2011, AJ, 141, 97
Woolf, V. M., & Wallerstein, G. 2005, MNRAS, 356, 963
Zacharias, N., Finch, C. T., Girard, T. M., et al. 2013, AJ, 145, 44